IEEE Access
Multidisciplinary | Rapid Review | Open Access Journal

Received November 11, 2019, accepted November 25, 2019, date of publication November 28, 2019,
date of current version December 13, 2019.

Digital Object Identifier 10.1109/ACCESS.2019.2956542

Performance Evaluation of Generalized Buffer-State-Based Relay Selection in NOMA-Aided Downlink

JUN KOCHI[1], (Student Member, IEEE), RYOTA NAKAI[2], (Student Member, IEEE), AND SHINYA SUGIURA[2], (Senior Member, IEEE)

[1]Department of Computer and Information Science, Tokyo University of Agriculture and Technology, Koganei 184-8588, Japan
[2]Institute of Industrial Science, The University of Tokyo, Meguro 153-8505, Japan

Corresponding author: Shinya Sugiura (sugiura@iis.u-tokyo.ac.jp)

This work was supported in part by the Japan Society for the Promotion of Science (JSPS) KAKENHI under Grant 16KK0120, Grant 17H03259, and Grant 19J22461, in part by the Japan Science and Technology Agency (JST) PRESTO under Grant JPMJPR1933, and in part by the Special Fund of the Institute of Industrial Science, The University of Tokyo.

ABSTRACT In this paper, we propose a novel buffer-state-based (BSB) non-orthogonal multiple access (NOMA)-aided downlink scheme for a two-hop cooperative network supporting multiple relay and destination nodes. More specifically, in the broadcast phase, the source node broadcasts information packets to multiple selected relay nodes. In the relaying phase, a selected relay node transmits packets to multiple destination nodes based on the NOMA principle. Here, the use of buffer at the relay nodes allows us to achieve a flexible relay selection. Furthermore, with the aid of buffer-state-based relay selection, the detrimental effects of empty- and full-buffer states are avoided. The theoretical outage probability and average packet delay are derived for our proposed scheme, based on the Markov-chain model. Our simulation results demonstrate that the proposed scheme outperforms the existing max-link and BSB relay selection benchmarks.

INDEX TERMS Broadcast, buffer, Markov chain, non-orthogonal multiple access (NOMA), outage probability, packet delay, successive interference cancellation, theoretical bound.

I. INTRODUCTION

The cooperative communications [1], [2] allow us to mitigate the detrimental effects of the propagation loss and multipath induced fading. The original cooperative systems did not rely on data buffers of relay nodes, where the maximum achievable performance is limited due to the predetermine end-to-end path. In order to combat this limitation, the family of buffer-aided relay selection was proposed [3]–[11], which allows more flexible scheduling of transmissions and receptions at the relay nodes, hence achieving higher reliability. However, buffering information packets in the buffers of the relay nodes naturally imposes an extra end-to-end packet delay.

The max-link protocol [5] was proposed in the context of two-hop buffer-aided cooperative networks. In this scheme, the single most reliable link out of all available links is selected in each time slot. While the max-link protocol achieves a high diversity order, which is equal to the number of links, the average packet delay significantly increases. In [6], the max-link protocol was extended to buffer-state-based (BSB) relay selection for the sake of avoiding a buffer overflow as well as an empty buffer. This allows us to attain a lower average packet delay and a better outage probability than the max-link counterpart. In [8], the simultaneous use of multiple source-to-relay (SR) links was proposed for reducing the packet delay, which is achievable by exploiting the broadcast nature of wireless channels. Moreover, inspired by both the protocols of [8] and [6], the generalized buffer-state-based (GBSB) relay selection protocol was proposed in [11]. This scheme is capable of achieving a lower average packet delay than the BSB scheme while achieving almost the same good outage probability as that of the BSB scheme. In [12], the GBSB scheme was further extended to that supporting information-theoretic secure communications exploiting physical layer security.

In recent years, motivated by the classic superposition coding [13], non-orthogonal multiple access (NOMA) has been extensively investigated as a means of guaranteeing ultra-high connectivity [14]–[21]. In contrast to the conventional orthogonal multiple access (OMA) counterpart, NOMA is capable of multiplexing signals of multiple users in the same

The associate editor coordinating the review of this manuscript and approving it for publication was Omer Chughtai.

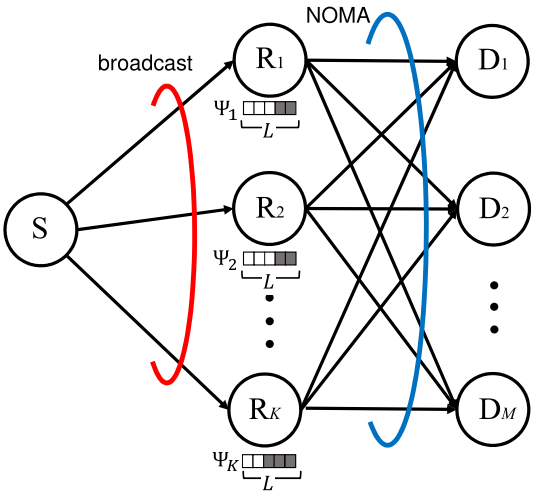

FIGURE 1. The system model of the proposed two-hop buffer-aided cooperative NOMA downlink, which is designed for simultaneously exploiting multiple SR links in the broadcast phase.

communication resources. At the receivers, the multiplexed signals are decoupled with the aid of successive interference cancellation (SIC) [22], to efficiently decode information of interest. There have been several relay selection schemes for cooperative NOMA downlink, where the relay nodes do not rely on data buffers [23]–[25]. Furthermore, in order to improve the achievable performance, the concept mentioned above of buffer-aided relay selection was incorporated into the cooperative NOMA systems in the two-user scenario [26]–[30]. More specifically, in [26], the adaptive buffer-aided relay selection scheme was proposed for the scenarios, where full- and partial-channel state information (CSI) of relay-to-destination (RD) links is available. In [27], the optimal mode selection scheme that maximizes the sum rate of the two NOMA users was presented. In [28], [30], the adaptive relay selection algorithm was proposed for the multiple-relay NOMA, for the sake of reducing the average delay without the sacrifice of the achievable diversity gain. Also, in [29], the hybrid NOMA and OMA buffer-aided relay selection was proposed, which switches the two multiple-access modes, in order to avoid an outage event.

Against the background, as mentioned above, the novel contribution of this paper is that we propose a buffer-aided cooperative NOMA downlink with a relay selection algorithm based on GBSB protocol [11]. While in the conventional buffer-aided NOMA schemes, the number of destination nodes is limited to two [26], [28], [29], our proposed scheme does not impose such a limitation. More specifically, we propose power allocation that minimizes the outage probability for the scenarios of the arbitrary number of the destination nodes. Moreover, we derive the theoretical bounds of the outage probability and the average packet delay for the proposed scheme. In our simulations, it is demonstrated that the proposed scheme exhibits better performance than the conventional buffer-aided schemes, such as the max-link protocol [5] and the BSB protocol [6].

The remainder of this paper is organized as follows. In Section II, we present the system model of the proposed scheme. In Section III, the theoretical values of the outage probability and the average packet delay are derived. Then we provide our performance results and discussions in Section IV. Finally, we conclude our paper in Section V.

II. SYSTEM MODEL

We consider a two-hop relaying network, consisting of a single source node S, K relay nodes R_k ($1 \leq k \leq K$), and M destination nodes D_m ($1 \leq m \leq M$), as shown in Fig. 1. We assume that there is no direct link between the source and the destination nodes, and that the relay nodes operate in the half-duplex mode, based on the decode-and-forward principle. Each relay node R_k has a data buffer of a finite size L. At maximum, M packets are stored in each buffer slot, and hence LM packets can be stored at each relay node.[1] The number of full buffer slots of the kth relay node is represented by Ψ_k ($0 \leq \Psi_k \leq L$). Furthermore, all the channels obey independent and identically distributed (IID) Rayleigh fading, where the channel coefficients are the random variables, following the Gaussian distribution with a zero mean. We also assume that in each time slot, CSI of all the links and the buffer states of relay nodes are collected by a central coordinator, similar to [8], [9], [11]. Based on the collected CSI, the central coordinator activates single or multiple links. For example, a base station may act as a central coordinator.[2]

In each time slot, either of the SR broadcast phase or the RD NOMA-based relaying phase is activated, based on the relay selection algorithm employed. More specifically, in the SR broadcast phase, the source node broadcasts M packets, corresponding to the M destination nodes, to the subset of the relay nodes. In the RD NOMA-based relaying phase, a single relay node is selected for simultaneously transmitting a packet to each of the M destinations, based on the power-domain NOMA principle [14]. If each destination node successfully decodes the received packet, an acknowledge (ACK) packet is sent back to all the relay nodes with stable low-rate feedback links. The target transmission rate for each destination node is fixed to r_0 [bps/Hz].

A. SOURCE-TO-RELAY BROADCAST PHASE

The channel capacity of the kth SR link is given by [8]

$$C_{\mathrm{SR}_k} = \frac{1}{2}\log_2(1 + \beta_{\mathrm{R}_k}|h_{\mathrm{SR}_k}|^2), \tag{1}$$

where h_{SR_k} denotes the channel coefficient and β_{R_k} denotes the associated average signal-to-noise ratio (SNR). Note that

[1] More specifically, in most of the previous buffer-aided relay selection schemes without NOMA, only a single destination node was considered, while in the proposed NOMA downlink, the number of destination nodes is M, where a source node simultaneously transmits a set of M packets to relay nodes. Hence, each of the L buffer slots is assumed to store M packets, for the sake of simplicity.

[2] To elaborate a little further, the distributed and the partially distributed implementations shown in [7], [8], [10] may reduce the overhead imposed by CSI acquisitions. Further detailed investigations are left for future studies.

since we assume the half-duplex mode for the relay nodes, a prelog factor of $1/2$ is multiplied in the capacity formula (1). If the capacity (1) is lower than the target transmission rate Mr_0 [bits/Hz], the associated link is in outage. Hence, the outage probability of the kth SR link is formulated by [8]

$$P_{\text{out}}^{\text{SR}_k} = \Pr\left[C_{\text{SR}_k} < Mr_0\right]. \tag{2}$$

Also, when the buffer Ψ_k of the kth relay node is full (i.e., $\Psi_k = L$), the associated SR link is unavailable, since the kth relay node cannot store any additional packets.

B. RELAY-TO-DESTINATION NOMA-BASED RELAYING PHASE

When the kth relay node is selected for carrying out NOMA-based relaying to the M destination nodes, the transmitted packet is constituted by superimposing M packets as follows:

$$x = \sum_{m=1}^{M} \sqrt{a_m} x_m, \tag{3}$$

where x_m denotes an information symbol for the mth destination node D_m with the power constraint of $\mathbb{E}[|x_m|^2] = 1$. Furthermore, a_m ($0 \le a_m \le 1$) represents the power allocation coefficients for the mth symbol x_m, where we have the relationship of

$$\sum_{m} a_m = 1. \tag{4}$$

Then, the packet received at the mth destination node is given by

$$y_m = h_{\text{R}_k\text{D}_m}\sqrt{P_r}x + n_m, \tag{5}$$

where $h_{\text{R}_k\text{D}_m}$ denotes the channel coefficient of the link between the kth relay node and the mth destination node, and P_r is the transmit power of the kth relay node. Also, the RD subset links associated with the kth relay node are defined by $\boldsymbol{h}_{\text{R}_k\text{D}} = [h_{\text{R}_k\text{D}_1}, \cdots, h_{\text{R}_k\text{D}_M}]^T$. Furthermore, n_m denotes the additive noise component at the mth destination node.

Without loss of generality, let us assume the relationship of

$$|h_{\text{R}_k\text{D}_1}| \ge |h_{\text{R}_k\text{D}_2}| \ge \cdots \ge |h_{\text{R}_k\text{D}_M}|, \tag{6}$$

since we consider IID channels in this paper. The multiplexed symbols are decoded based on SIC in descending order, i.e., from x_M to x_i at the ith destination node, where the ith destination node D_i has to decode other $M - i$ symbols x_m ($m > i$), before decoding its own symbol x_i [14].

Here, let us consider that the ith destination node successfully decoded $M - m$ symbols, i.e., $x_{m+1}, \cdots, x_M$ ($m \ge i$), which are removed from the received packet x with the aid of SIC. Then, the corresponding instantaneous signal-to-interference-and-noise ratio (SINR) for the ith destination node to decode the mth symbol x_m is expressed as

$$\gamma_{i\to m}^{\text{R}_k} = \begin{cases} \dfrac{a_m P_r |h_{\text{R}_k\text{D}_i}|^2}{P_r \sum_{j=1}^{m-1} a_j |h_{\text{R}_k\text{D}_i}|^2 + \sigma_{\text{D}}^2} & \text{for } m \ge i > 1 \\ \dfrac{a_1 P_r |h_{\text{R}_k\text{D}_1}|^2}{\sigma_{\text{D}}^2} & \text{for } m = i = 1, \end{cases} \tag{7}$$

where we have the noise power of σ_{D}^2 at the destination node. From (6) and (7), we have the relationship of

$$\gamma_{i\to m}^{\text{R}_k} \ge \gamma_{m\to m}^{\text{R}_k} \quad \text{for } m \ge i. \tag{8}$$

Let us define that when each of the M destination nodes successfully decodes its own packet, the associated event is not outage. Hence, the outage probability for the event, where the kth relay node is selected for packet transmissions is represented by

$$P_{\text{out}}^{\text{R}_k\text{D}} = \Pr\left[\frac{1}{2}\log_2\left(1 + \min_{m\ge i}\{\gamma_{i\to m}^{\text{R}_k}\}\right) < r_0\right]. \tag{9}$$

Furthermore, based on (8) and (9) is simplified to

$$P_{\text{out}}^{\text{R}_k\text{D}} = \Pr\left[\frac{1}{2}\log_2\left(1 + \min_{m}\{\gamma_{m\to m}^{\text{R}_k}\}\right) < r_0\right]. \tag{10}$$

Note that, when the buffer of the kth relay node R_k is empty, i.e., $\Psi_k = 0$, the associated kth RD subset links are unavailable.

C. POWER ALLOCATION OF NOMA-BASED RELAYING PHASE

Based on the CSI collected, the central coordinator calculates the power allocation coefficients a_m ($1 \le m \le M$). From (10), the NOMA-based packet transmissions of the kth relay node become successful, when we have

$$\gamma_{i\to m}^{\text{R}_k} \ge \gamma_t \quad \text{for } m \ge i, \tag{11}$$

where

$$\gamma_t = 2^{2r_0} - 1. \tag{12}$$

Based on (7) and (4), the condition for the successful transmissions (11) is rewritten by

$$a_i \ge \begin{cases} \dfrac{\gamma_t(\sum_{j=1}^{i-1} a_j \delta |h_{\text{R}_k\text{D}_i}|^2 + 1)}{\delta |h_{\text{R}_k\text{D}_i}|^2} & \text{for } m \ge i > 1 \\ \dfrac{\gamma_t}{\delta |h_{\text{R}_k\text{D}_1}|^2} & \text{for } m = i = 1, \end{cases} \tag{13}$$

where we have $\delta = P_r/\sigma_{\text{D}}^2$. In order to achieve successful packet transmissions from the kth relay node to the M destination nodes, there have to be the power allocation factors $\mathbf{a} = [a_1, \cdots, a_M]^T \in \mathcal{R}^M$, which satisfies both the relationships of (13) and (4). Otherwise, the corresponding transmission event becomes outage.

Hence, we arrive at the power allocation factors of

$$a_i = \begin{cases} \dfrac{\omega\gamma_t(\sum_{j=1}^{i-1} a_j \delta |h_{\text{R}_k\text{D}_i}|^2 + 1)}{\delta |h_{\text{R}_k\text{D}_i}|^2} & \text{for } i > 1 \\ \dfrac{\omega\gamma_t}{\delta |h_{\text{R}_k\text{D}_1}|^2} & \text{for } i = 1, \end{cases} \tag{14}$$

where the normalization factor $\omega \in \mathcal{R}$ is determined, such that the power constraint (4) is satisfied. As above-mentioned, in order to achieve successful packet transmissions, (13) and (4) have to be satisfied, which is equivalent to the relationship of

$$\omega \ge 1. \tag{15}$$

TABLE 1. Priority classification.

Priority	Low	Middle	High
SR links h_{SR_k}	$\Psi_k = L-1$	$1 < \Psi_k < L-1$	$\Psi_k = 0, 1$
RD link subsets $\boldsymbol{h}_{\mathrm{R}_k\mathrm{D}}$	$\Psi_k = 1$	—	$\Psi_k \geq 2$

In order to expound a little further, in the link selection process, a central coordinator activates a single link or multiple links by sending control packets, similar to [3]–[11]. Hence, the calculated power allocation factors are conveyed from the central coordinator to the relay nodes together with the control packets, when a NOMA-based relaying phase is activated. This does not impose any substantial additional overhead in comparison to the conventional schemes [3]–[11].

D. LINK SELECTION ALGORITHM

The proposed link selection algorithm is carried out in two steps. In the first step, depending on the buffer states of the relay nodes, the central coordinator categorizes the priority of each of the SR links h_{SR_k} and of the RD link subsets $\boldsymbol{h}_{\mathrm{R}_k\mathrm{D}}$, based on Table 1. More specifically, the priority of the kth SR link h_{SR_k} is categorized as low for $\Psi_k = L-1$, middle for $1 < \Psi_k < L-1$, and high for $\Psi_k = 0, 1$, respectively. Similarly, the priority of the kth RD link subsets $\boldsymbol{h}_{\mathrm{R}_k\mathrm{D}}$ is categorized as low for $\Psi_k = 1$ and high for $\Psi_k \geq 2$, respectively.

In the second step, the SR links and RD link subsets are selected. Firstly, the SR links and RD link subsets that induce an outage event are excluded from the candidates to be selected, based on (2) and (10). Then, the link selection is carried out from the available links, according to our algorithm of Table 2. Here, the stable SR link or RD link subset tends to be selected, such that the full or empty buffer states are avoided. Also, the number of occupied buffer slots of each relay node is maintained to be as low as possible in the range of $\Psi_k \geq 2$. This is for the sake of maintaining the achievable diversity order to be high and the average delay to be low, similar to [11]. Let us define the number of available low-, middle-, and high-priority SR links as $N_{\mathrm{SR}}^{\mathrm{low}}$, $N_{\mathrm{SR}}^{\mathrm{middle}}$, and $N_{\mathrm{SR}}^{\mathrm{high}}$, respectively. Similarly, the number of available low- and high-priority RD link subsets is defined as $N_{\mathrm{RD}}^{\mathrm{low}}$ and $N_{\mathrm{RD}}^{\mathrm{high}}$, respectively. More specifically, in Case 1, $N_{\mathrm{SR}}^{\mathrm{middle}}$ middle-priority and $N_{\mathrm{SR}}^{\mathrm{high}}$ high-priority SR links are activated, while in Case 3 $N_{\mathrm{SR}}^{\mathrm{middle}}$ middle-priority SR links are selected, in order to broadcast M information packets to each activated relay node. In Case 2, a single out of $N_{\mathrm{RD}}^{\mathrm{high}}$ high-priority RD link subset associated with the $\arg\max_k \left(\min_m\{\gamma_{m\to m}^{\mathrm{R}_k}\}\right)$th relay node is activated for NOMA-based packet transmissions to the M destination nodes. Similarly, in Case 4, a single out of $N_{\mathrm{RD}}^{\mathrm{low}}$ low-priority RD link subset is selected. In Case 5, a single highest-capacity out of $N_{\mathrm{SR}}^{\mathrm{low}}$ low-priority SR links is activated. Furthermore, in Case 6, there are no available links, hence resulting in the outage event.

Note that the calculation complexity required for the central coordinator to carry out link selection is constitute by the priority classification of Table 1, the K calculations of $(1/2)\log_2(1+\beta_{\mathrm{R}_k}|h_{\mathrm{SR}_k}|^2)$ $(k = 1, \cdots, K)$ in (1), and the K calculations of $(1/2)\log_2\left(1+\min_m\{\gamma_{m\to m}^{\mathrm{R}_k}\}\right)$ $(k = 1, \cdots, K)$ in (10). Hence, the calculation complexity of the proposed scheme is as low as those of the conventional buffer-aided relay selection schemes [3]–[11].

To exemplify the proposed link selection algorithm, consider a simplified scenario of $K = 2$ relay nodes, each having the buffer of $L = 3$, and $M = 2$ destination nodes. Also, assume that the buffers of the first and the second relay nodes are $\Psi_1 = 2$ and $\Psi_2 = 1$, respectively. Then, according to Table 1, the priorities of SR links associated with the first and the second relay nodes are classified to be low and high, respectively. Similarly, the priorities of the RD link subsets related to the first and the second relay nodes are set to high and low, respectively. Finally, according to Table 2, we arrive at Case 1, where the SR link associated with the second relay node is activated.

III. DERIVATION OF THEORETICAL BOUNDS

In this section, we derive the theoretical bounds of the outage probability and the average packet delay for the proposed scheme. Our analysis is based on the Markov chain model. However, since the proposed scheme is based on NOMA-aided relaying, the derivation is not identical to those of the previous buffer-aided schemes relying on the SR broadcast channels [8], [11]. For simplicity, we only consider the scenario of $K = 2$ relay nodes, each having an $(L = 2)$-sized buffer, as well as $M = 3$ destination nodes. However, the presented derivation is readily applicable to arbitrary parameters of K, L, and M. In this scenario, the total number of buffer states is $N_{\mathrm{state}} = 19$, as listed in Table 3, where at maximum four symbols, i.e., ◯, □, △, and ◇, are considered.

Fig. 2 shows the state transition diagram of the Markov chain in the proposed scheme. Note that the six states of $s_{13}, s_{15}, s_{16}, s_{17}, s_{18}$, and s_{19} are unreachable from the initial empty-buffer state s_1.

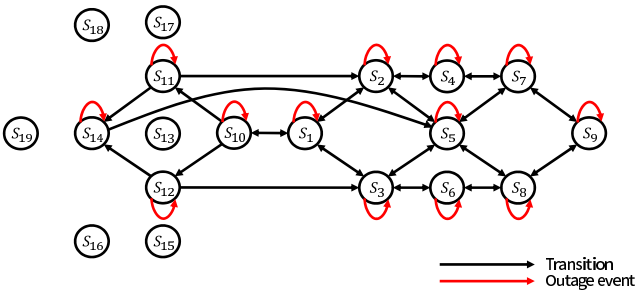

FIGURE 2. State transition diagram of the Markov chain model representing proposed system with $K = 2$ relay nodes employing $(L = 2)$-sized buffers.

A. ANALYTICAL OUTAGE PROBABILITY

By substituting (1) into (2), the outage probability of the kth SR link is rewritten by

$$P_{\mathrm{out}}^{\mathrm{SR}_k} = 1 - \Pr\left[|h_{\mathrm{SR}_k}|^2 \geq \frac{2^{6r_0}-1}{\beta_{\mathrm{R}_k}}\right]. \tag{16}$$

TABLE 2. Link selection algorithm.

	$N_{\mathrm{SR}}^{\mathrm{low}}$	$N_{\mathrm{SR}}^{\mathrm{middle}}$	$N_{\mathrm{SR}}^{\mathrm{high}}$	$N_{\mathrm{RD}}^{\mathrm{low}}$	$N_{\mathrm{RD}}^{\mathrm{high}}$	Selected links
Case 1	—	—	≥ 1	—	—	$N_{\mathrm{SR}}^{\mathrm{high}} + N_{\mathrm{SR}}^{\mathrm{middle}}$ high- and middle-priority SR links
Case 2	—	—	0	—	≥ 1	A high-priority RD link subset associated with the $\arg\max_k \left(\min_m\{\gamma_{m\to m}^{\mathrm{R}_k}\}\right)$th relay node
Case 3	—	≥ 1	0	—	0	$N_{\mathrm{SR}}^{\mathrm{middle}}$ middle-priority SR links
Case 4	—	0	0	≥ 1	0	A low-priority RD link subset associated with the $\arg\max_k \left(\min_m\{\gamma_{m\to m}^{\mathrm{R}_k}\}\right)$th relay node
Case 5	≥ 1	0	0	0	0	A single low-priority SR link
Case 6	0	0	0	0	0	Outage event

TABLE 3. Legitimate buffer states for $K = 2$ relay node employing ($L = 2$)-sized buffers [11].

States	Relay 1		Relay 2	
s_1	empty	empty	empty	empty
s_2	○	empty	empty	empty
s_3	empty	empty	○	empty
s_4	○	□	empty	empty
s_5	○	empty	□	empty
s_6	empty	empty	○	□
s_7	○	△	□	empty
s_8	○	empty	□	△
s_9	○	△	□	◇
s_{10}	○	empty	○	empty
s_{11}	○	△	○	empty
s_{12}	○	empty	○	△
s_{13}	○	△	○	△
s_{14}	○	△	○	□
s_{15}	○	empty	□	○
s_{16}	○	△	□	○
s_{17}	□	○	○	empty
s_{18}	□	○	○	△
s_{19}	□	○	△	○

Since the channel coefficient h_{SR_k} is a random variable, following the Gaussian distribution, (16) is modified to

$$P_{\mathrm{out}}^{\mathrm{SR}_k} = 1 - \int_{\frac{2^{2r_0}-1}{\beta_{\mathrm{R}_k}}}^{\infty} \frac{1}{\Omega_{\mathrm{SR}}} \exp(-\frac{x}{\Omega_{\mathrm{SR}}})dx = 1 - \exp\left(-\frac{2^{6r_0}-1}{\Omega_{\mathrm{SR}}\beta_{\mathrm{R}_k}}\right), \tag{17}$$

where Ω_{SR} is the variance of the SR channel coefficients h_{SR_k} $(k = 1, \cdots, K)$.

Similar to Section II, without loss of generality, let us assume again $|h_{\mathrm{R}_k\mathrm{D}_1}|^2 \geq |h_{\mathrm{R}_k\mathrm{D}_2}|^2 \geq |h_{\mathrm{R}_k\mathrm{D}_3}|^2$. Then, based on (14) and (15), the probability that the kth relay node successfully transmit M packets to the M destination nodes is given by

$$\frac{\gamma_t}{\delta x}(1 + 2\gamma_t + {\gamma_t}^2) + \frac{\gamma_t}{\delta y}(1 + \gamma_t) + \frac{\gamma_t}{\delta z} \leq 1, \tag{18}$$

where we define $x = |h_{\mathrm{R}_k\mathrm{D}_1}|^2$, $y = |h_{\mathrm{R}_k\mathrm{D}_2}|^2$, and $z = |h_{\mathrm{R}_k\mathrm{D}_3}|^2$ for the sake of simplicity. Furthermore, (18) is modified to

$$z \geq \frac{\rho xy}{xy - \rho x(1+\gamma_t) - \rho y(1 + 2\gamma_t + {\gamma_t}^2)}, \tag{19}$$

where $\rho = \gamma_t/\delta$. Since $y \geq z$, we obtain

$$y \geq \frac{\rho xy}{xy - \rho x(1+\gamma_t) - \rho y(1 + 2\gamma_t + {\gamma_t}^2)}, \tag{20}$$

i.e.,

$$y \geq \frac{\rho x(\gamma_t + 2)}{x - \rho(1 + 2\gamma_t + {\gamma_t}^2)}. \tag{21}$$

Because of $|h_1|^2 \geq |h_2|^2$, we also have

$$x \geq \frac{\rho x(\gamma_t + 2)}{x - \rho(1 + 2\gamma_t + {\gamma_t}^2)}, \tag{22}$$

i.e.,

$$x \geq \rho(3 + 3\gamma_t + {\gamma_t}^2). \tag{23}$$

Similar to (17), under the condition that the kth relay node is selected for NOMA-based packet transmissions, the probability that the outage event does not occur is formulated by

$$P_{1_{\mathrm{suc}}}^{\mathrm{R}_k D} = \int_x \int_y \int_z \frac{1}{\Omega_{\mathrm{R}_k\mathrm{D}_3}} \exp(-\frac{z}{\Omega_{\mathrm{R}_k\mathrm{D}_3}})dz \times \frac{1}{\Omega_{\mathrm{R}_k\mathrm{D}_2}} \exp(-\frac{y}{\Omega_{\mathrm{R}_k\mathrm{D}_2}})dy \times \frac{1}{\Omega_{\mathrm{R}_k\mathrm{D}_1}} \exp(-\frac{x}{\Omega_{\mathrm{R}_k\mathrm{D}_1}})dx, \tag{24}$$

which is calculated over the range of (19), (21), and (23). Furthermore, $\Omega_{\mathrm{R}_k\mathrm{D}_1}$, $\Omega_{\mathrm{R}_k\mathrm{D}_2}$, and $\Omega_{\mathrm{R}_k\mathrm{D}_3}$ denote the variance of the channel coefficients $h_{\mathrm{R}_k\mathrm{D}_1}$, $h_{\mathrm{R}_k\mathrm{D}_2}$, and $h_{\mathrm{R}_k\mathrm{D}_3}$, respectively.

Hence, the outage probability for the packet transmissions from the kth relay node to the M destination nodes is formulated by

$$P_{\mathrm{out}}^{\mathrm{R}_k D} = 1 - \sum P_{i_{\mathrm{suc}}}^{\mathrm{R}_k D}. \tag{25}$$

Having obtained the analytical outage probability for each link and link subset selection in (17) and (25), now we derive the analytical average outage probability. Let us denote Ξ_n and Ξ_n^a by the set of legitimate links that are available in terms of buffer states and the set of available links that are not outage in terms of packet transmissions, respectively, under the state s_n. Hence, we have the relationship of $\Xi_n^a \subset \Xi_n$ [11]. Furthermore, we define the state transition matrix of the Markov model of Fig. 2 by $\mathbf{A} \in \mathcal{R}^{N_{\mathrm{state}} \times N_{\mathrm{state}}}$. The pth-row and

qth-column element of A indicates the transition probability from the state s_q to the state s_p, which is represented by

$$\mathrm{A}_{pq} = \sum_{\Xi_q^a \subset \Xi_q} \Pr\left[\Xi_q^a\right] \Pr\left[s_q \to s_p | \Xi_q^a\right]. \tag{26}$$

Moreover, $\Pr\left[\Xi_q^a\right]$ is the probability that a subset Ξ_q^a successfully convey packets, which is expressed by

$$\Pr\left[\Xi_q^a\right] = \prod_{h_{\mathrm{SR}_k} \in \Xi_q^a} \left(1 - P_{\mathrm{out}}^{\mathrm{SR}_k}\right) \prod_{h_{\mathrm{SR}_k} \in \Xi_q, h_{\mathrm{SR}_k} \notin \Xi_q^a} P_{\mathrm{out}}^{\mathrm{SR}_k} \prod_{\boldsymbol{h}_{\mathrm{R}_k\mathrm{D}} \in \Xi_q^a} \left(1 - P_{\mathrm{out}}^{\mathrm{R}_k\mathrm{D}}\right) \prod_{\boldsymbol{h}_{\mathrm{R}_k\mathrm{D}} \in \Xi_q, \boldsymbol{h}_{\mathrm{R}_k\mathrm{D}} \notin \Xi_q^a} P_{\mathrm{out}}^{\mathrm{R}_k\mathrm{D}}. \tag{27}$$

Also, $\Pr[s_q \to s_p | \Xi_q^a]$ is the transition probability from the state s_q to the state s_p under the link condition of Ξ_q^a.

The steady-state probabilities $\boldsymbol{\pi} = [\pi_1, \cdots, \pi_{N_{\mathrm{state}}}]^T \in \mathcal{R}^{N_{\mathrm{state}}}$ is given by [5]

$$\boldsymbol{\pi} = (A - I + B)^{-1} b. \tag{28}$$

Finally, since the qth diagonal element of $\mathbf{A}$ represents the outage probability, under the condition of the state s_q. Hence, the average outage probability is formulated by

$$P_{\mathrm{out}} = \mathrm{diag}(A)\boldsymbol{\pi}. \tag{29}$$

B. ANALYTICAL AVERAGE PACKET DELAY

The average packet delay in the network consists of the delay at the source node and that at the relay nodes, which are represented, respectively, by $\mathbb{E}[D_{\mathrm{S}}]$ and $\mathbb{E}[D_{\mathrm{R}}]$. Based on Littles' law [31], the average packet delay at a node t is given by

$$\mathbb{E}[D_t] = \frac{\mathbb{E}[\Psi_t]}{\eta_t}, \tag{30}$$

where $\mathbb{E}[\Psi_t]$ denotes the average queuing length and η_t denotes the throughput at the node t. Note that in our two-hop network, if the source node transmits sufficiently high number of packets, the system's average throughput is given by

$$\eta = \frac{(1 - P_{\mathrm{out}})}{2}. \tag{31}$$

Souce packets are queued only when the source node is selected to for transmissions, leading to $\eta_{\mathrm{S}} = \mathbb{E}[\Psi_{\mathrm{S}}]$. Hence, we have [11]

$$\mathbb{E}[D_{\mathrm{S}}] = 1. \tag{32}$$

Furthermore, since the probability that each relay node is selected for the packet transmissions is the same, the throughput of each relay node is also the same. Hence, we have

$$\eta_R = \frac{\eta}{K} = \frac{1 - P_{\mathrm{out}}}{2K}. \tag{33}$$

Furthermore, the average queuing length at the relay nodes $\mathbb{E}[\Psi_R]$ is equal to the average of the number of different packets stored at the relay nodes' buffers over all the states, which is given by

$$\mathbb{E}[\Psi_R] = \frac{1}{N} \sum_{i=1}^{N_{\mathrm{state}}} \pi_i \Psi(i), \tag{34}$$

where $\Psi(i)$ is the number of different packets stored at the relay nodes in the state s_i. Hence, the average packet delay at the relay nodes is

$$\mathbb{E}[\Psi_R] = \frac{\mathbb{E}[\Psi_R]}{\eta_R} = \frac{2}{1 - P_{\mathrm{out}}} \sum_{i=1}^{N_{\mathrm{state}}} \pi_i \Psi(i). \tag{35}$$

Finally, from (32) and (35), the average packet delay of the system is given by

$$\mathbb{E}[D] = \mathbb{E}[D_{\mathrm{S}}] + \mathbb{E}[D_{\mathrm{R}}] \tag{36}$$

$$= 1 + \frac{2}{1 - P_{\mathrm{out}}} \sum_{i=1}^{N_{\mathrm{state}}} \pi_i \Psi(i). \tag{37}$$

IV. PERFORMANCE RESULTS

In this section, we present our simulation results in order to evaluate the achievable performance of the proposed scheme, which is compared with the max-link protocol [5] and the BSB protocol [6]. Since the max-link and BSB schemes are not originally designed for NOMA-based downlink, we herein modify them for the presented two-hop NOMA-based downlink scenario. More specifically, in the max-link scheme, from the highest SR link $\max_k\{h_{\mathrm{SR}_k}\}$ and the highest minimum RD subset channels $\max_k\{\min(|\boldsymbol{h}_{\mathrm{R}_k\mathrm{D}}|)\}$, the higher one is selected to be activated in each time slot. Furthermore, in the BSB scheme, the above-mentioned max-link scheme is extended to that supporting the buffer-state-based link selection of Section II-D. For simplicity, we assumed that the transmission rate of each node was maintained to be $r_0 = 1$ [bps/Hz] while retaining the number of the destination nodes to be $M = 3$. Moreover, we assumed that the buffers of all the relay nodes are empty in their initial condition of our simulations. A sufficiently long source frame of packets is generated in each Monte Carlo simulation, in order to attain a steady-state. In our simulations, more than 10^5 packets were generated for calculating each numerical curve, which is sufficiently long according to [11]. Also, the variance of the SR and RD links is set to $\Omega_{\mathrm{SR}} = \Omega_{\mathrm{R}_k\mathrm{D}} = 1$. Their average SNRs are assumed to be identical, i.e., $\gamma = \beta_{\mathrm{R}_k} = \delta$.

In Fig.3, we compared the numerical and theoretical results of the proposed scheme, where the number of relay nodes was set to $K = 2$, each having an $(L = 2)$-sized buffer. More specifically, Figs. 3(a) and 3(b) show the outage probability and the average delay, respectively. It was found that the numerical and theoretical results matched well, and hence, the system model considered in this paper was validated.

Fig. 4 shows the outage probabilities of the three protocols, where the number of relay nodes was given by $K = 3$ and 6, each supporting an $(L = 2)$-sized buffer. The average SNR was varied from $\gamma = 10$ to 30 dB. For $K = 3$, the proposed

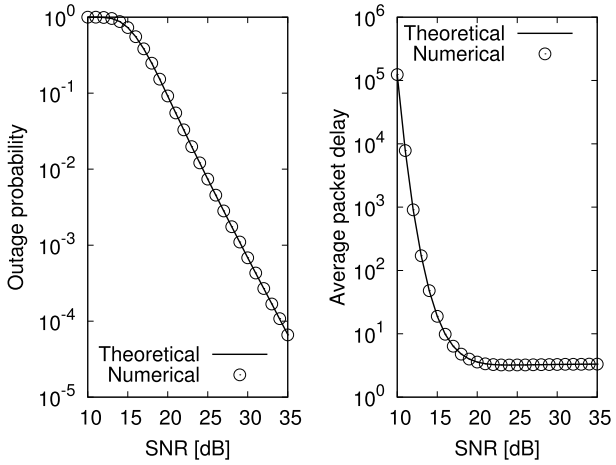

(a) Outage probability (b) Average packet delay

FIGURE 3. Numerical and theoretical results of the proposed scheme with $K = 2$ relay nodes with the buffer size of $L = 2$, while we varied the average SNR from γ from 10 to 35.

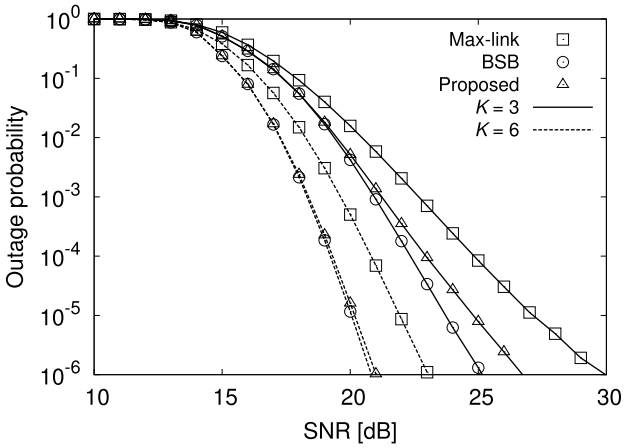

FIGURE 4. Outage probabilities of the proposed, the max-link, and the BSB schemes, where we considered $(K, L) = (3, 10)$ and $(6, 10)$, while the average SNR was varied from $\gamma = 10$ to 30 dB.

scheme outperformed the max-link scheme, while exhibiting slightly worse performance than the BSB scheme. Furthermore, for $K = 6$, the proposed scheme achieved approximately the best performance, which is close to that of the BSB scheme. To provide further insights, the BSB benchmark scheme typically exhibits the best outage probability performance among the existing buffer-aided relay selection family, as mentioned in [6], [11]. The proposed scheme was found to achieve the nearly lowest outage probability comparable to the BSB scheme.

Figs. 5(a) and 5(b) show the average packet delay for the average SNRs of $\gamma = 15$ dB and 30 dB, respectively, where the number of relay nodes was varied from $K = 2$ to 10 with the buffer size of $L = 10$. In Fig. 5(a), the BSB and the proposed schemes exhibited the comparable lowest delay profile, which decreased upon increasing the number of relay nodes. This is because the increased number of relay nodes contributes to the increase of the achievable diversity order.

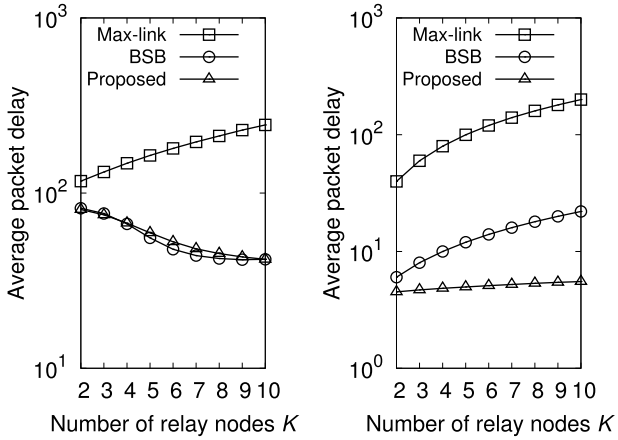

(a) $\gamma = 15$ dB (b) $\gamma = 30$ dB

FIGURE 5. Average packet delays of the proposed, the max-link, and the BSB schemes, where the number of the relay nodes was varied from $K = 2$ to 10, each having an $(L = 10)$-sized buffer. The average SNR was given by $\gamma = 15$, and 30 dB.

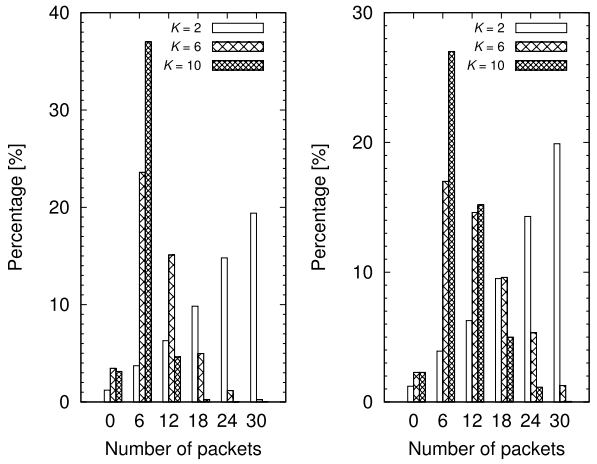

(a) BSB protocol (b) Proposed protocol

FIGURE 6. Distribution of the number of packets stored at each relay node in the proposed scheme and the BSB scheme, where the number of the relay nodes was given by K to 2, 6, and 10, each having an $(L = 10)$-sized buffer, and the average SNR was set to $\gamma = 15$ dB.

Moreover, in Fig. 5(b), the proposed scheme attained the lowest packet delay among the three schemes. Upon increasing the number of relay nodes, the proposed scheme's performance advantages over the max-link and BSB benchmark schemes increased.

Figs. 6(a) and 6(b) show the distributions of the number of packets stored at the relay nodes in the proposed and the BSB schemes, respectively, where the number of relay nodes was given by $K = 2$, 6, and 10, each equipped with an $(L = 10)$-sized buffer. The average SNR was maintained to be $\gamma = 15$ dB. Observe in Figs. 6(a) and 6(b) that the average number of packets stored at the relay nodes decreased, upon increasing the number of relay nodes for both the schemes. This contributes to avoiding the detrimental effects of buffer overflow as well as to maintaining the average delay to be small.

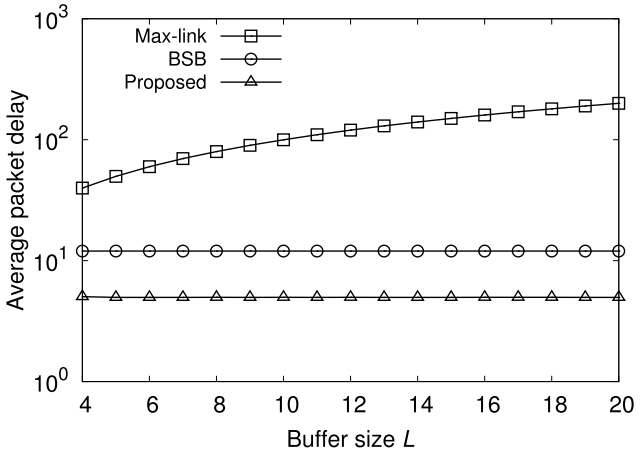

FIGURE 7. Average packet delays of the proposed, the max-link and the BSB schemes, where we considered $K = 5$ relay nodes and the average SNR of $\gamma = 30$ dB, while the buffer size was varied from $L = 2$ to 20.

Finally, Fig. 7 shows the average packet delay of the three schemes for the average SNR of $\gamma = 30$ dB, where the buffer size was varied from $L = 4$ to 20, while maintaining the number of relay nodes to be $K = 5$. It was found in Fig. 7 that the average packet delay of the proposed scheme achieved the best performance. More specifically, the average packet delay of the proposed protocol remained constant since our algorithm is designed for maintaining the number of packets stored at the relay nodes to be as low as possible.

Note that in this paper, we considered only NOMA mode for the relaying phase. However, this may not be necessarily beneficial, especially when the channel gains of RD links are not sufficiently high. To combat this limitation, the concept of hybrid NOMA/OMA relaying [29], [30] may be readily applicable to our scheme. Alternatively, it may also be beneficial to adapt the number of destination nodes, depending on the channel qualities. However, these are beyond the scope of this paper, and detailed investigations are left for future studies.

We assumed in our simulations that perfect CSI and the buffer states are periodically collected by a central coordinator. However, such information may be out-of-date, depending on the channel's coherence time. In such a case, the activated link does not perform as well as expected. Additionally, the overhead required for the central coordinator to collect CSI and the buffer states may be substantially high in a rapidly fading scenario. The proposed scheme and other conventional buffer-aided relay selection schemes may suffer from these detrimental factors, which are left for future studies.

V. CONCLUSION

In this paper, we proposed the buffer-state-based relay selection scheme for a two-hop NOMA-based downlink network, consisting of multiple relay and destination nodes. For the sake of exploiting the merits of data buffers, the source node broadcasts information packets to multiple relay nodes, which is useful for reducing the average packet delay. Furthermore, we proposed a dynamic power allocation scheme for the NOMA downlink, which minimizes the outage probability. Additionally, the theoretical outage probability and average delay were derived for our scheme. Our simulation results demonstrated that the proposed scheme is capable of achieving better outage probability and average packet delay than the max-link and BSB benchmark schemes.

REFERENCES

[1] A. Nosratinia, T. E. Hunter, and A. Hedayat, "Cooperative communication in wireless networks," *IEEE Commun. Mag.*, vol. 42, no. 10, pp. 74–80, Oct. 2004.
[2] S. Sugiura, S. X. Ng, L. Kong, S. Chen, and L. Hanzo, "Quasi-synchronous cooperative networks: A practical cooperative transmission protocol," *IEEE Veh. Technol. Mag.*, vol. 7, no. 4, pp. 66–76, Dec. 2012.
[3] B. Xia, Y. Fan, J. Thompson, and H. V. Poor, "Buffering in a three-node relay network," *IEEE Trans. Wireless Commun.*, vol. 7, no. 11, pp. 4492–4496, Nov. 2008.
[4] N. Zlatanov, A. Ikhlef, T. Islam, and R. Schober, "Buffer-aided cooperative communications: Opportunities and challenges," *IEEE Commun. Mag.*, vol. 52, no. 4, pp. 146–153, Apr. 2014.
[5] I. Krikidis, T. Charalambous, and J. S. Thompson, "Buffer-aided relay selection for cooperative diversity systems without delay constraints," *IEEE Trans. Wireless Commun.*, vol. 11, no. 5, pp. 1957–1967, May 2012.
[6] S. Luo and K. C. Teh, "Buffer state based relay selection for buffer-aided cooperative relaying systems," *IEEE Trans. Wireless Commun.*, vol. 14, no. 10, pp. 5430–5439, Oct. 2015.
[7] V. Jamali, N. Zlatanov, H. Shoukry, and R. Schober, "Achievable rate of the half-duplex multi-hop buffer-aided relay channel with block fading," *IEEE Trans. Wireless Commun.*, vol. 14, no. 11, pp. 6240–6256, Nov. 2015.
[8] M. Oiwa and S. Sugiura, "Reduced-packet-delay generalized buffer-aided relaying protocol: Simultaneous activation of multiple source-to-relay links," *IEEE Access*, vol. 4, pp. 3632–3646, 2016.
[9] M. Oiwa, C. Tosa, and S. Sugiura, "Theoretical analysis of hybrid buffer-aided cooperative protocol based on max-max and max-link relay selections," *IEEE Trans. Veh. Technol.*, vol. 65, no. 11, pp. 9236–9246, Nov. 2016.
[10] M. Najafi, V. Jamali, and R. Schober, "Optimal relay selection for the parallel hybrid RF/FSO relay channel: Non-buffer-aided and buffer-aided designs," *IEEE Trans. Commun.*, vol. 65, no. 7, pp. 2794–2810, Jul. 2017.
[11] R. Nakai, M. Oiwa, K. Lee, and S. Sugiura, "Generalized buffer-state-based relay selection with collaborative beamforming," *IEEE Trans. Veh. Technol.*, vol. 67, no. 2, pp. 1245–1257, Feb. 2018.
[12] R. Nakai and S. Sugiura, "Physical layer security in buffer-state-based max-ratio relay selection exploiting broadcasting with cooperative beamforming and jamming," *IEEE Trans. Inf. Forensics Security*, vol. 14, no. 2, pp. 431–444, Feb. 2019.
[13] T. Cover, "Broadcast channels," *IEEE Trans. Inf. Theory*, vol. IT-18, no. 1, pp. 2–14, Jan. 1972.
[14] Y. Liu, Z. Qin, M. Elkashlan, Z. Ding, A. Nallanathan, and L. Hanzo, "Nonorthogonal multiple access for 5G and beyond," *Proc. IEEE*, vol. 105, no. 12, pp. 2347–2381, Dec. 2017.
[15] Z. Ding, Y. Liu, J. Choi, Q. Sun, M. Elkashlan, C.-L. I, and H. V. Poor, "Application of non-orthogonal multiple access in LTE and 5G networks," *IEEE Commun. Mag.*, vol. 55, no. 2, pp. 185–191, Feb. 2017.
[16] L. Dai, B. Wang, Y. Yuan, S. Han, C.-L. I, and Z. Wang, "Non-orthogonal multiple access for 5G: Solutions, challenges, opportunities, and future research trends," *IEEE Commun. Mag.*, vol. 53, no. 9, pp. 74–81, Sep. 2015.
[17] Z. Ding, Z. Yang, P. Fan, and H. V. Poor, "On the performance of non-orthogonal multiple access in 5G systems with randomly deployed users," *IEEE Signal Process. Lett.*, vol. 21, no. 12, pp. 1501–1505, Dec. 2014.
[18] Z. Ding, M. Peng, and H. V. Poor, "Cooperative non-orthogonal multiple access in 5G systems," *IEEE Commun. Lett.*, vol. 19, no. 8, pp. 1462–1665, Aug. 2015.
[19] S. Timotheou and I. Krikidis, "Fairness for non-orthogonal multiple access in 5G systems," *IEEE Signal Process. Lett.*, vol. 22, no. 10, pp. 1647–1651, Oct. 2015.
[20] F. Liu, P. Mähönen, and M. Petrova, "Proportional fairness-based power allocation and user set selection for downlink NOMA systems," in *Proc. IEEE ICC*, Kuala Lumpur, Malaysia, May 2016, pp. 1–6.

[21] M. Najafi, V. Jamali, P. D. Diamantoulakis, G. K. Karagiannidis, and R. Schober, "Non-orthogonal multiple access for FSO backhauling," in *Proc. IEEE WCNC*, Barcelona, Spain, Apr. 2018, pp. 1–6.
[22] P. Patel and J. Holtzman, "Analysis of a simple successive interference cancellation scheme in a DS/CDMA system," *IEEE J. Sel. Areas Commun.*, vol. 12, no. 5, pp. 796–807, Jun. 1994.
[23] Z. Ding, H. Dai, and H. V. Poor, "Relay selection for cooperative NOMA," *IEEE Wireless Commun. Lett.*, vol. 5, no. 4, pp. 416–419, Aug. 2016.
[24] P. Xu, Z. Yang, Z. Ding, and Z. Zhang, "Optimal relay selection schemes for cooperative NOMA," *IEEE Trans. Veh. Technol.*, vol. 67, no. 8, pp. 7851–7855, Aug. 2018.
[25] Y. Li, Y. Li, X. Chu, Y. Ye, and H. Zhang, "Performance analysis of relay selection in cooperative NOMA networks," *IEEE Commun. Lett.*, vol. 23, no. 4, pp. 760–763, Apr. 2019.
[26] Q. Zhang, Z. Liang, Q. Li, and J. Qin, "Buffer-aided non-orthogonal multiple access relaying systems in Rayleigh fading channels," *IEEE Trans. Commun.*, vol. 65, no. 1, pp. 95–106, Jan. 2017.
[27] S. Luo and K. C. Teh, "Adaptive transmission for cooperative NOMA system with buffer-aided relaying," *IEEE Commun. Lett.*, vol. 21, no. 4, pp. 937–940, Apr. 2017.
[28] N. Nomikos, T. Charalambous, D. Vouyioukas, G. K. Karagiannidis, and R. Wichman, "Relay selection for buffer-aided non-orthogonal multiple access networks," in *Proc. IEEE Globecom Workshops*, Singapore, Dec. 2017, pp. 1–6.
[29] N. Nomikos, T. Charalambous, D. Vouyioukas, G. K. Karagiannidis, and R. Wichman, "Hybrid NOMA/OMA with buffer-aided relay selection in cooperative networks," *IEEE J. Sel. Topics Signal Process.*, vol. 13, no. 3, pp. 524–537, Jun. 2019.
[30] M. Alkhawatrah, Y. Gong, G. Chen, S. Lambotharan, and J. A. Chambers, "Buffer-aided relay selection for cooperative NOMA in the Internet of Things," *IEEE Internet Things J.*, vol. 6, no. 3, pp. 5722–5731, Jun. 2019.
[31] Z. Tian, G. Chen, Y. Gong, Z. Chen, and J. A. Chambers, "Buffer-aided max-link relay selection in amplify-and-forward cooperative networks," *IEEE Trans. Veh. Technol.*, vol. 64, no. 2, pp. 553–565, Feb. 2015.

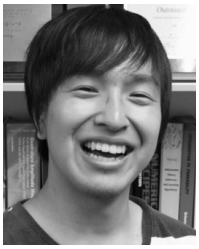

JUN KOCHI received the B.E. degree in computer and information sciences from the Tokyo University of Agriculture and Technology, Koganei, Japan, in 2019, where he is currently pursuing the master's degree. His research interest is in non-orthogonal multiple access.

RYOTA NAKAI (S'17) received the B.E. and M.E. degrees in computer and information sciences from the Tokyo University of Agriculture and Technology, Koganei, Japan, in 2017 and 2019, respectively. He is currently pursuing the Ph.D. degree with the Institute of Industrial Science, The University of Tokyo.

His research interests are in cooperative wireless communications and physical layer security. He received the IEEE VTS Tokyo Chapter 2017 Young Researcher's Encouragement Award.

SHINYA SUGIURA (M'06–SM'12) received the B.S. and M.S. degrees in aeronautics and astronautics from Kyoto University, Kyoto, Japan, in 2002 and 2004, respectively, and the Ph.D. degree in electronics and electrical engineering from the University of Southampton, Southampton, U.K., in 2010.

From 2004 to 2012, he was a Research Scientist with the Toyota Central Research and Development Laboratories, Inc., Aichi, Japan. From 2013 to 2018, he was an Associate Professor with the Department of Computer and Information Sciences, Tokyo University of Agriculture and Technology, Koganei, Japan. Since 2018, he has been an Associate Professor with the Institute of Industrial Science, The University of Tokyo, Tokyo, Japan, where he heads the Wireless Communications Research Group. In 2019, he was recognized as The University of Tokyo Excellent Young Researcher. He has a cross-appointment as a PRESTO Researcher, Japan Science and Technology Agency. He has authored or coauthored more than 70 IEEE journal articles. His research has covered a range of areas in wireless communications, networking, signal processing, and antenna technology.

Dr. Sugiura was a recipient of numerous awards, including the 2008 IEEE Antennas and Propagation Society Japan Chapter Young Engineer Award, the Sixth IEEE Communications Society Asia-Pacific Outstanding Young Researcher Award, in 2011, the 13th Ericsson Young Scientist Award, in 2011, the 28th Telecom System Technology Award from the Telecommunications Advancement Foundation, in 2013, the 14th Funai Information Technology Award (First Prize) from the Funai Foundation, in 2015, the Sixth RIEC Award from the Foundation for the Promotion of Electrical Communication, in 2016, the Young Scientists' Prize by the Minister of Education, Culture, Sports, Science and Technology of Japan, in 2016, and the Fifth Yasuharu Suematsu Award, in 2019. He was also certified as an Exemplary Reviewer for the IEEE COMMUNICATIONS LETTERS, in 2013 and 2014, and the IEEE TRANSACTIONS ON COMMUNICATIONS, in 2018. He is currently serving as an Editor of the IEEE WIRELESS COMMUNICATIONS LETTERS.